Enhancing Alzheimer's Disease Detection Using Advanced MRI Preprocessing and Deep Learning Techniques

Bandaru A. Chakravarthi
Department of Computer Science and Engineering, Koneru Lakshmaiah Education Foundation, Hyderabad, Telangana, India
bandaruachakravarthi@gmail.com

Gandla Shivakanth
Department of Computer Science and Engineering, Koneru Lakshmaiah Education Foundation, Hyderabad, Telangana, India
shvkanth0@gmail.com (corresponding author)

Received: 16 October 2025 | Revised: 6 November 2025 and 11 November 2025 | Accepted: 15 November 2025

 DOI: https://doi.org/10.48084/etasr.15572

ABSTRACT

This study investigates how optimized Magnetic Resonance Imaging (MRI) preprocessing enhances the performance of Artificial Intelligence (AI) models for Alzheimer's Disease (AD) detection. A standardized preprocessing pipeline, comprising noise reduction, skull stripping, and intensity normalization, was integrated into a hybrid Deep Learning (DL) model called MRI-Net. MRI-Net combines Convolutional Neural Networks (CNNs), Recurrent Neural Networks (RNNs), Long Short-Term Memory (LSTM), and Vision Transformers (ViTs) to leverage complementary spatial and contextual information. Using the publicly available ADNI dataset, MRI-Net achieved a classification accuracy of 94.7%, surpassing baseline CNN (88.2%), CNN+RNN (90.5%), and ViT (92.8%) models. The inclusion of a structured preprocessing pipeline improved anatomical clarity, reduced inter-subject variability, and enhanced feature discriminability. These findings demonstrate that optimized preprocessing substantially strengthens model generalization and diagnostic reliability. The proposed MRI-Net framework highlights the importance of integrating preprocessing and hybrid AI architectures to support early-stage AD detection and clinical decision-making.

Keywords-Alzheimer's disease detection; MRI preprocessing; machine learning; deep learning; feature engineering; biomarkers; medical imaging; diagnostic accuracy

I. INTRODUCTION

Alzheimer's Disease (AD) is a progressive neurodegenerative disorder that impairs memory, cognition, and behavior, posing a growing global healthcare challenge. Early diagnosis is vital to improve patient outcomes and slow disease progression. Among diagnostic modalities, brain MRI plays a significant role in revealing structural and functional alterations linked to AD, offering non-invasive, high-resolution neuroanatomical insights [1, 2]. AI advancement has revolutionized MRI analysis, enabling the detection of subtle biomarkers through Machine Learning (ML) and DL models [3, 4]. However, the reliability of these models depends heavily on preprocessing, which mitigates noise, removes non-brain tissue, and standardizes image intensities to ensure consistent feature extraction [5]. Despite its importance, preprocessing remains underexplored due to challenges in scanner variability, patient heterogeneity, and computational demand [6, 7].

Techniques such as Gaussian smoothing and non-local means filtering enhance structural clarity [8-10], while skull stripping and intensity normalization standardize anatomical representation across subjects [6, 11, 12]. Dimensionality reduction and augmentation strategies further improve robustness and reduce overfitting [13, 14]. CNN-based architectures have effectively captured AD biomarkers, such as hippocampal volume and cortical thickness [15, 16], and hybrid CNN–SVM and CNN–RF models have improved interpretability and accuracy [17]. Attention mechanisms and ViTs have enhanced explainability by focusing on clinically relevant brain regions [13, 18].

However, inconsistencies in MRI preprocessing pipelines, coupled with the computational burden of atlas-based normalization, hinder reproducibility and clinical scalability [19-22]. Addressing these limitations requires standardized, efficient, and generalizable frameworks.

The present study proposes MRI-Net, a hybrid AI framework that unifies optimized preprocessing with the CNN, LSTM, and ViT components for robust AD detection. Its key contributions include: (1) a standardized, computationally efficient MRI preprocessing pipeline; (2) a hybrid model integrating voxel-level, temporal, and spatial features; and (3) an evaluation strategy quantifying preprocessing impact on diagnostic performance. MRI-Net, thus, bridges the gap between preprocessing optimization and clinically translatable AI-based AD detection.

II. METHODOLOGY

A. Methodology Overview

This study investigates how optimized MRI preprocessing can enhance AD detection through advanced AI models. The proposed MRI-Net framework integrates state-of-the-art preprocessing techniques with hybrid DL components, including CNNs, RNNs with LSTM units, and ViTs for efficient analysis of structural MRI data. The overall workflow, illustrated in Figure 1, begins with MRI acquisition and preprocessing, and culminates in AI-based classification of AD.

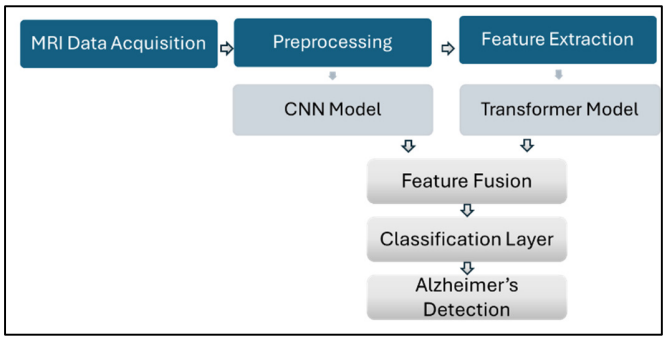

Fig. 1. Workflow of the proposed framework.

Representative slices of the ADNI MRI scans are shown in Figure 2, depicting the progression from raw input to smoothed output, with each stage successively enhancing anatomical clarity and preparing the data for subsequent feature extraction and model training.

B. Dataset Details

The dataset was obtained from the AD Neuroimaging Initiative (ADNI) [23], which provides high-resolution T1-weighted structural MRI scans of subjects at different stages of AD. After quality control (baseline scans only, complete diagnostic labels, and artifact removal), the final dataset comprised 1,200 subjects: 400 AD, 400 MCI, and 400 Cognitively Normal (CN) participants. Stratified sampling ensured balanced classes across subsets: 80 % (960 images) for training, 10 % (120) for validation, and 10 % (120) for testing. The random seed was fixed at 42 for reproducibility.

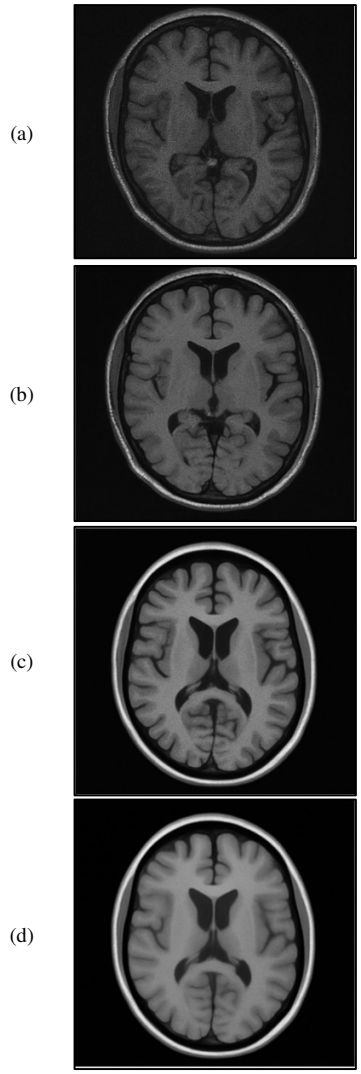

Fig. 2. Representative ADNI MRI slices showing: (a) raw image, (b) image after noise reduction, (c) skull-stripped image, and (d) smoothed image.

To improve generalization, data augmentation was applied only to the training set using:

- Rotation ±10°
- Horizontal and vertical flips (probability = 0.5)
- Translation ±5 pixels
- Addition of low-level Gaussian noise ($\sigma = 0.01$)

All MRI volumes were resampled to 1 mm³ voxel spacing and intensity-normalized as described below.

C. Preprocessing Techniques

1) Intensity Normalization

Normalization reduces inter-subject intensity variation and stabilizes training. Each image I was standardized using z-score normalization:

$$I_{norm}(x,y) = \frac{I(x,y) - \mu}{\sigma} \quad (1)$$

2) Noise Reduction

A non-local means or small Gaussian kernel (σ = 1 voxel) filter was used to preserve fine hippocampal structures while suppressing scanner noise. Larger kernels commonly used in prior ADNI studies tend to blur these boundaries; hence, the smaller σ improves regional contrast.

3) Skull Stripping

Non-brain tissue was removed using FSL-BET with a fractional intensity threshold of 0.30, followed by automated quality control. The conservative threshold prevents cortical erosion observed in more aggressive settings.

4) Segmentation and Smoothing

After skull stripping, Regions of Interest (ROIs), principally the hippocampus and entorhinal cortex, were segmented for subsequent morphometric analysis. Smoothing was applied to enhance the signal-to-noise ratio using a Gaussian filter:

$$I_{smooth}(x,y) = \sum_{i,j} I(x-i, y-j) \cdot G(i.j,\sigma) \quad (2)$$

where $G(i.j,\sigma)$ is the Gaussian kernel function with a standard deviation σ used to smooth the image.

5) Morphometric Feature Extraction

Two complementary descriptors were derived:

- Voxel-Based Morphometry (VBM): VBM quantifies voxel-wise gray-matter concentration variations, sensitive to local atrophy.
- Surface-Based Morphometry (SBM): SBM evaluates cortical thickness and surface-area metrics that reflect neurodegenerative progression.

D. Hybrid Deep-Learning Architecture (MRI-Net)

MRI-Net combines CNN, RNN/LSTM, and ViT modules to leverage complementary spatial, temporal, and contextual information.

1) CNN

CNN layers extract hierarchical spatial features through convolution and pooling. The convolution operation is defined as:

$$f(x,y) = (I * K)(x,y) = \sum_m \sum_n I(m,n) \cdot K(x-m, y-n) \quad (3)$$

where I is the input image, K is the kernel, and (x, y) represents the coordinates of the output feature map.

2) RNN / LSTM Component

The RNN with LSTM units captures longitudinal progression patterns across temporal MRI sequences, effectively modeling disease evolution over multiple time points.

3) ViT Module

The ViT divides MRI slices into fixed-size patches and applies self-attention to model spatial dependencies between regions. The attention mechanism enhances the feature representation of complex cortical relationships.

4) Fusion Strategy

Outputs from the CNN, LSTM, and ViT are concatenated and passed through fully connected gating layers to form the final diagnostic embedding used by the classifier.

E. Training Configuration

The dataset was split into 80:10:10 (train, validation, test) subsets with class balance maintained. Training used binary cross-entropy loss:

$$L = -\frac{1}{N} + \sum_{i=1}^{N} [\![y_i \, log\,(\hat{y}_i) + \,(1-y_i)\, log(1-\hat{y}_i)]\!] \quad (4)$$

where N is the number of samples, y_i is the actual label, and $\hat{y}_i$ is the predicted probability. The Adam optimizer (learning rate = 1×10^{-4}) was employed with a batch size of 32, dropout rate of 0.5, and weight decay of 1×10^{-5}. Early stopping (patience = 10 epochs) prevented overfitting. All models were initialized with a random seed of 42 for reproducibility.

F. Evaluation Metrics

Model performance was assessed using accuracy, precision, recall, F1-score, and Area Under the ROC Curve (AUC-ROC). Accuracy measures overall correctness, Precision and recall evaluate the model's ability to detect positives while avoiding false negatives, F1-score balances these metrics, and AUC-ROC quantifies discrimination capability.

G. Computational Environment

Experiments were conducted on a high-performance workstation equipped with:

- GPU: NVIDIA RTX 3090 (24 GB VRAM)
- CPU: Intel Xeon Gold 6248R @ 3.00 GHz
- Memory: 128 GB DDR4 RAM
- Storage: 1 TB NVMe SSD
- Operating System: Ubuntu 20.04 LTS

The software stack included TensorFlow 2.6.0 with Keras, FSL for preprocessing, and Scikit-learn for dataset splitting and evaluation.

III. RESULTS

A. Classification Performance and Impact of Preprocessing

MRI-Net achieved strong classification performance after the inclusion of the preprocessing pipeline. On the ADNI test set, MRI-Net reached 94.7% accuracy, outperforming the baseline CNN (88.2%), CNN+RNN (90.5%), and ViT (92.8%). Precision, recall, and F1-score consistently reflect this improved performance. The inclusion of structured preprocessing appears to be a key factor in this performance gain.

To understand the performance of the model, it is important to consider how the specific preprocessing methods influenced these results. Generally, processing medical images could be complex and noisy, with several artifacts and very low contrast

between normal and abnormal tissues. The MRI-Net model incorporated steps in noise reduction and skull stripping, which led to higher performance. Without preprocessing, the base model's accuracy was only 85.1%. This highlights the necessity of preprocessing.

Figure 3 illustrates the performance metrics of various models evaluated for AD detection, with baseline accuracies of 88.2% for CNN, 90.5% for CNN+RNN, 92.8% for ViT, and 94.7% for MRI-Net. This supports the model's readiness for integration into clinical decision support systems. This conclusion emphasizes that the merit of the model does not lie merely in its ability to correctly diagnose the disease but also in the minimization of false positives and negatives and, thus, is adaptable for clinical use.

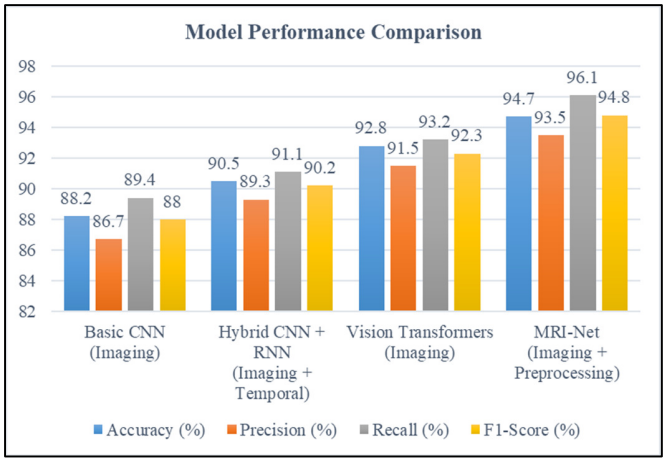

Fig. 3. Model performance comparison on the ADNI test set (n = 120).

The precision and recall of the model are particularly exceptional. With 93.5% precision and 96.1% recall, the model is effective in minimizing false positives (precision) and capturing as many relevant instances as possible (recall). The F1-score further reinforces this balance, indicating reliability and consistency with true positives while minimizing errors with a score of 94.8%.

At the same time, the necessity of pre-processing for boosting performance turns out to be important. While the basic CNN reached an accuracy of 88.2% using only imagery data, other models, which include temporal features or advanced preprocessing techniques, outperform this basic model. The hybrid CNN + RNN model, which uses both imaging and temporal data, was able to reach an accuracy of 90.5%, while ViTs reached 92.8%. MRI-Net, combining robust preprocessing with deep feature modeling, consistently outperformed all other configurations. It was the actual practice that determined how crucial preprocessing was in enhancing the diagnostic value of this model.

The MRI-Net model was consistent in its performance throughout the training process, as can be seen in the learning curves for training and validation accuracy and loss. It was observed that from the very first epoch to the last, there was an upward trend in accuracy and a steady decline in loss, meaning that the model was learning from the data properly and generalizing well to new, unseen data. As shown in Figure 4, the performance of the model improved significantly in the first few epochs. The training accuracy increased from 72.1% to 94.7% at epoch 20, and validation accuracy also demonstrated a similar trend. Validation accuracy nearly followed the training accuracy, which indicates that the model generalized well without overfitting. This is an important aspect when applying the model to clinical environments where unseen data can pose challenges.

The validation loss decreased gradually and reached a final value of 0.14 at epoch 20, as displayed in Figure 5, which also indicates that the model learned to make more accurate predictions as the epochs progressed. Steady loss reduction indicates that MRI-Net did not face problems, such as vanishing gradients, which is a common problem in DL models. These metrics were stable after epoch 15, suggesting early convergence and strong model stability.

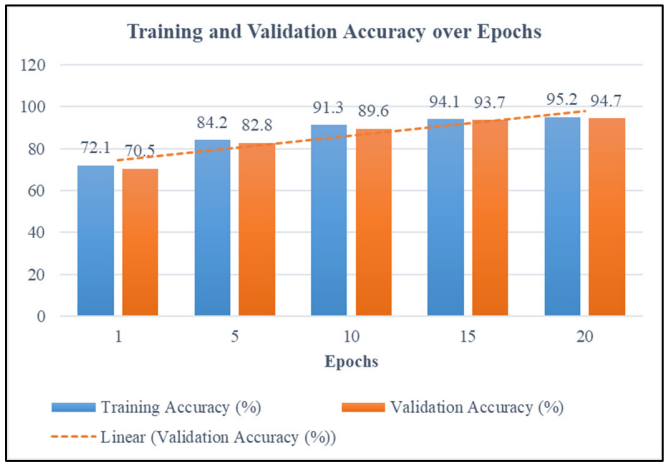

Fig. 4. Training and validation accuracy over epochs.

The stability within the validation metrics, as evidenced by the tiny gap between the performance of training and validation, implies that robust generalization happens. This would be critical to the medical imaging domain, since a model has to be efficient at handling unseen data reliably when making the distinction between a proper and improper diagnosis.

However, preprocessing techniques were strongly responsible for the model's high performance, as depicted in Figure 6. The MRI-Net model includes various important preprocessing operations, such as noise reduction and skull stripping. There are noises inevitably present in MRI images due to the devices employed to scan and the irrelevant areas from the background of such images. The impact of these preprocessing steps is well covered in the results.

The baseline model without preprocessing achieved 85.1% accuracy, as shown in Figure 6, highlighting the difficulty of learning from raw MRI data affected by noise and irrelevant features. Applying noise reduction improved accuracy to 88.5%, while skull stripping further increased it to 89.2% by

isolating brain regions of diagnostic relevance. When combined, these preprocessing steps raised accuracy to 94.7%, confirming their synergistic impact on model precision. Statistical validation using paired t-tests ($p < 0.01$) confirmed the significance of MRI-Net's improvement over baseline models. Attention and saliency visualizations also revealed focus on hippocampal and entorhinal regions, consistent with Alzheimer's pathology and clinical interpretability.

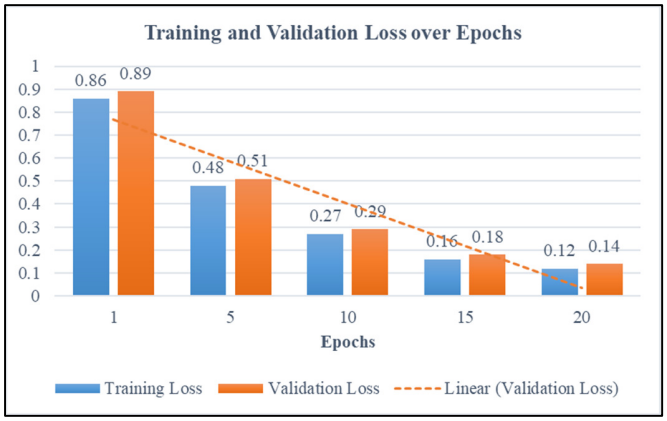

Fig. 5. Training and validation loss over epochs.

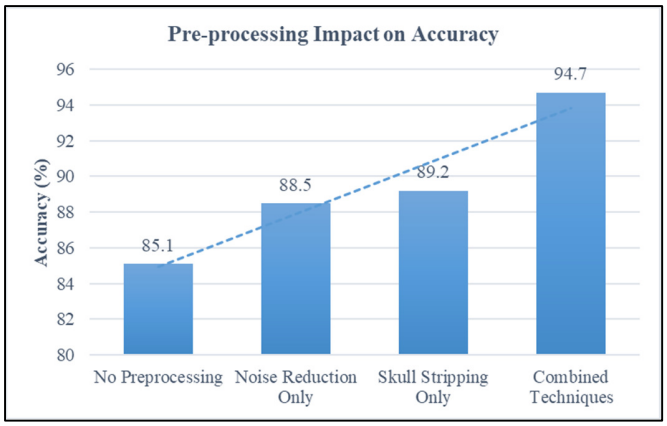

Fig. 6. Ablation analysis of preprocessing stages.

B. Limitations and Future Scope

While MRI-Net demonstrates strong diagnostic performance for Alzheimer's detection, its computationally intensive preprocessing limits real-time clinical deployment. Future work will focus on optimizing these processes for efficiency while preserving diagnostic precision. Although the model performs well on the ADNI dataset, its generalizability to other datasets and diverse populations remains to be validated. Expanding training data and exploring domain adaptation can enhance robustness across scanners and demographics. Further improvements in interpretability, such as integrating attention or saliency maps, and multimodal extensions with PET or CT imaging, will advance clinical trust and broaden the model's applicability in neurodegenerative disease diagnosis [24].

IV. CONCLUSION

The proposed hybrid Deep Learning (DL) architecture, MRI-Net, demonstrates strong performance in Alzheimer's disease (AD) detection, achieving an accuracy of 94.7%, which is 6.5% higher than the baseline Convolutional Neural Network (CNN) and 4.2% above Vision Transformer (ViT)-only models. This improvement results from the integration of advanced preprocessing techniques, such as noise reduction and skull stripping, with MRI-Net, which combines CNN, Recurrent Neural Network (RNN), and ViT modules. MRI-Net effectively combines spatial, temporal, and contextual learning to produce robust, clinically relevant feature representations. It maintains high precision (93.5%) and recall (96.1%), minimizing false negatives while ensuring diagnostic reliability. Future work will focus on enhancing generalization across diverse Magnetic Resonance Imaging (MRI) datasets, such as OASIS and AIBL, integrating multimodal imaging, such as PET or CT, and improving model interpretability and computational efficiency for clinical deployment. Overall, MRI-Net offers a balanced combination of accuracy, transparency, and scalability, positioning it as a promising framework for early-stage Alzheimer's diagnosis and real-time clinical applications.

DATA AVAILABILITY STATEMENT

The MRI dataset analyzed in the study is publicly available from the Alzheimer's Disease Neuroimaging Initiative (ADNI): https://adni.loni.usc.edu/data-samples/adni-data/neuroimaging/mri/mri-image-data-sets/.

CODE AVAILABILITY STATEMENT

The code and trained weights used in this study are available from the corresponding author upon reasonable request.

REFERENCES

[1] G. Battineni *et al.*, "Improved Alzheimer's Disease Detection by MRI Using Multimodal Machine Learning Algorithms," *Diagnostics*, vol. 11, no. 11, Nov. 2021, Art. no. 2103, https://doi.org/10.3390/diagnostics11112103.

[2] S. Ul Rehman *et al.*, "AI-based Tool for Early Detection of Alzheimer's Disease," *Heliyon*, vol. 10, no. 8, Apr. 2024, Art. no. e29375, https://doi.org/10.1016/j.heliyon.2024.e29375.

[3] A. A. A. El-Latif, S. A. Chelloug, M. Alabdulhafith, and M. Hammad, "Accurate Detection of Alzheimer's Disease Using Lightweight Deep Learning Model on MRI Data," *Diagnostics*, vol. 13, no. 7, Mar. 2023, Art. no. 1216, https://doi.org/10.3390/diagnostics13071216.

[4] D. M. Sima *et al.*, "Artificial Intelligence Assistive Software Tool for Automated Detection and Quantification of Amyloid-Related Imaging Abnormalities," *JAMA Network Open*, vol. 7, no. 2, Feb. 2024, Art. no. e2355800, https://doi.org/10.1001/jamanetworkopen.2023.55800.

[5] L. S. Saoud and H. AlMarzouqi, "Explainable Early Detection of Alzheimer's Disease Using ROIs and an Ensemble of 138 3D Vision Transformers," *Scientific Reports*, vol. 14, no. 1, Nov. 2024, Art. no. 27756, https://doi.org/10.1038/s41598-024-76313-0.

[6] L. Chen, H. Qiao, and F. Zhu, "Alzheimer's Disease Diagnosis with Brain Structural MRI Using Multiview-Slice Attention and 3D Convolution Neural Network," *Frontiers in Aging Neuroscience*, vol. 14, Apr. 2022, Art. no. 871706, https://doi.org/10.3389/fnagi.2022.871706.

[7] M. Khatun, M. M. Islam, H. Rahman Rifat, Md. S. Bin Shahid, Md. A. Talukder, and M. A. Uddin, "Hybridized Convolutional Neural Networks and Long Short-Term Memory for Improved Alzheimer's

Disease Diagnosis from MRI Scans," in *2023 26th International Conference on Computer and Information Technology*, Cox's Bazar, Bangladesh, Dec. 2023, pp. 1–6, https://doi.org/10.1109/ICCIT60459.2023.10441274.

[8] D. AlSaeed and S. F. Omar, "Brain MRI Analysis for Alzheimer's Disease Diagnosis Using CNN-Based Feature Extraction and Machine Learning," *Sensors*, vol. 22, no. 8, Apr. 2022, Art. no. 2911, https://doi.org/10.3390/s22082911.

[9] M. K. A, A. Gurung, and P. Ranjan, "Vision Mamba: Cutting-Edge Classification of Alzheimer's Disease with 3D MRI Scans." arXiv, 2024, https://doi.org/10.48550/ARXIV.2406.05757.

[10] Z. S. Aaraji and H. H. Abbas, "Automatic Classification of Alzheimer's Disease Using Brain MRI Data and Deep Convolutional Neural Networks." arXiv, Mar. 31, 2022, https://doi.org/10.48550/arXiv.2204.00068.

[11] X. Bi, W. Liu, H. Liu, and Q. Shang, "Artificial Intelligence-based MRI Images for Brain in Prediction of Alzheimer's Disease," *Journal of Healthcare Engineering*, vol. 2021, pp. 1–7, Oct. 2021, https://doi.org/10.1155/2021/8198552.

[12] N. Ntampakis, K. Diamantaras, I. Chouvarda, V. Argyriou, and P. Sarigianndis, "Introducing DEFORMISE: A Deep Learning Framework for Dementia Diagnosis in the Elderly Using Optimized MRI Slice Selection." arXiv, 2024, https://doi.org/10.48550/ARXIV.2407.17324.

[13] N. M. AbdelAziz, W. Said, M. M. AbdelHafeez, and A. H. Ali, "Advanced Interpretable Diagnosis of Alzheimer's Disease Using SECNN-RF Framework with Explainable AI," *Frontiers in Artificial Intelligence*, vol. 7, Sept. 2024, Art. no. 1456069, https://doi.org/10.3389/frai.2024.1456069.

[14] C. Mahanty *et al.*, "Effective Alzheimer's Disease Detection Using Enhanced Xception Blending with Snapshot Ensemble," *Scientific Reports*, vol. 14, no. 1, Nov. 2024, Art. no. 29263, https://doi.org/10.1038/s41598-024-80548-2.

[15] M. Heenaye-Mamode Khan, P. Reesaul, M. M. Auzine, and A. Taylor, "Detection of Alzheimer's Disease Using Pre-Trained Deep Learning Models Through Transfer Learning: A Review," *Artificial Intelligence Review*, vol. 57, no. 10, Sept. 2024, Art. no. 275, https://doi.org/10.1007/s10462-024-10914-z.

[16] S. Odimayo, C. C. Olisah, and K. Mohammed, "Structure Focused Neurodegeneration Convolutional Neural Network for Modelling and Classification of Alzheimer's Disease," *Scientific Reports*, vol. 14, no. 1, July 2024, Art. no. 15270, https://doi.org/10.1038/s41598-024-60611-8.

[17] H. A. Raza *et al.*, "A Proficient Approach for the Classification of Alzheimer's Disease Using a Hybridization of Machine Learning and Deep Learning," *Scientific Reports*, vol. 14, no. 1, Dec. 2024, Art. no. 30925, https://doi.org/10.1038/s41598-024-81563-z.

[18] T. Akan, S. Alp, and M. A. N. Bhuiyanb, "Vision Transformers and Bi-LSTM for Alzheimer's Disease Diagnosis from 3D MRI." arXiv, Jan. 06, 2024, https://doi.org/10.48550/arXiv.2401.03132.

[19] Y. Lin, X. Li, Y. Zhang, and J. Tang, "Attention-Based Efficient Classification for 3D MRI Image of Alzheimer's Disease," in *Proceedings of the 2023 6th International Conference on Sensors, Signal and Image Processing*, Nanjing, China, Oct. 2023, pp. 34–39, https://doi.org/10.1145/3653863.3653865.

[20] H. Givian, J.-P. Calbimonte, and for the Alzheimer's Disease Neuroimaging Initiative, "Early Diagnosis of Alzheimer's Disease and Mild Cognitive Impairment Using MRI Analysis and Machine Learning Algorithms," *Discover Applied Sciences*, vol. 7, no. 1, Dec. 2024, Art. no. 27, https://doi.org/10.1007/s42452-024-06440-w.

[21] R. Maity *et al.*, "Early Detection of Alzheimer's Disease in Structural and Functional MRI," *Frontiers in Medicine*, vol. 11, Dec. 2024, Art. no. 1520878, https://doi.org/10.3389/fmed.2024.1520878.

[22] S. Tascedda *et al.*, "Advanced AI Techniques for Classifying Alzheimer's Disease and Mild Cognitive Impairment," *Frontiers in Aging Neuroscience*, vol. 16, Nov. 2024, Art. no. 1488050, https://doi.org/10.3389/fnagi.2024.1488050.

[23] C. R. Jack *et al.*, "Overview of ADNI MRI," *Alzheimer's & Dementia*, vol. 20, no. 10, pp. 7350–7360, Oct. 2024, https://doi.org/10.1002/alz.14166.

[24] B. K. Raghupathy, M. R. Reddy, Prasad Theeda, E. Balasubramanian, R. K. Namachivayam, and M. Ganesan, "Harnessing Explainable Artificial Intelligence (XAI) based SHAPLEY Values and Ensemble Techniques for Accurate Alzheimer's Disease Diagnosis," *Engineering, Technology & Applied Science Research*, vol. 15, no. 2, pp. 20743–20747, Apr. 2025, https://doi.org/10.48084/etasr.9619.